Self-aligned growth of carbon nanosticks

D Kölbl[1], J Ebbecke[1,2], A Heinrich[3] and A Wixforth[1]

[1] Experimentalphysik I, Institut für Physik der Universität Augsburg, Universitätsstraße 1, 86135 Augsburg, Germany
[2] School of Engineering and Physical Sciences, Heriot-Watt University, Edinburgh, EH14 4AS, UK
[3] Experimentalphysik IV, Institut für Physik der Universität Augsburg, Universitätsstraße 1, 86135 Augsburg, Germany

Abstract
Pulsed laser deposition of carbon on $LiNbO_3$ as substrate material leads for certain process parameters to the growth of self-aligned carbon stick-like nanoparticles (so called nanosticks). The carbon nanosticks and the growth conditions were investigated in detail by means of atomic force microscopy, scanning electron microscopy and conductivity measurements. A model for the growth mechanism is presented on the basis of the experimental investigations.

1. Introduction

Self-organization of nanostructures, the so called 'bottom-up' approach, is expected to play an important role in future nanoelectronics. Especially, the combination of self-organization and subsequent nanolithography offers new functionality and can reduce the costs of device fabrication significantly. This symbiosis can even be enhanced if the self-organized nanostructures have a preferential growth direction. Examples of self-aligned growth methods are vertical growth of carbon nanotubes and semiconductor nanowires [1–4].

In this paper, we present a method to grow horizontally aligned carbon nanosticks (CNS) on a piezo and pyroelectric substrate material by pulsed laser deposition (PLD). The growth process is investigated in detail and a model for the aligned self-organization effect is presented.

2. Nanostick growth and experimental investigations

$LiNbO_3$ (rotation 128°, Y-cut, X propagation) was used as a substrate material. PLD (KrF laser, 248 nm) was applied to create a plasma (C, C_2, C_3, ...) [5, 6] by focusing the laser onto a target of pure graphite. The sample was glued to a sample holder and slowly heated up under vacuum. The growth conditions are presented in table 1.

Three examples of the structures obtained under these conditions are shown as scanning electron microscope (SEM) pictures in figure 1. Clearly visible is the directed growth of the nanosticks and the different size distribution. Also a capture zone (highlighted with a dashed rectangle) around each CNS can be seen in figure 1(a) [7]. In figure 1(b) a picture of CNS with higher resolution is presented. The inset of figure 1(b) is a small sketch of a sample after the PLD process indicating that the growth of CNS occurs only very close to the edge (0–0.5 mm) of the substrate material. This schematic sketch is verified with an SEM image of the bottom sample edge at lower magnification presented in figure 1(c). The position of figure 1(c) is marked with a rectangle in figure 1(b).

Table 1. Parameter range for the pulsed laser deposition of carbon nanosticks.

Parameter	Value
KrF laser	$\lambda = 248$ nm
Energy per pulse	800 mJ
Pulse length	20 ns
Number of pulses	100–1000
Gas atmosphere	Argon/oxygen
Pressure	0.1–0.4 mbar
Sample temperature	500–700 °C

In order to evaluate the importance of the substrate on the growth process the substrates were glued to the sample holder with two different orientations as sketched in figures 2(a) and (c). After the PLD process the samples were covered with a thin conductive metal layer and SEM inspection was used to verify the growth direction. The results are shown in figures 2(b) and (d). The pictures exhibit that the CNS always grow perpendicular to the $LiNbO_3$ X-axis independent of the orientation in which they were glued to the heated sample holder. This result proves the assumption that the substrate properties play an important role for the certain growth

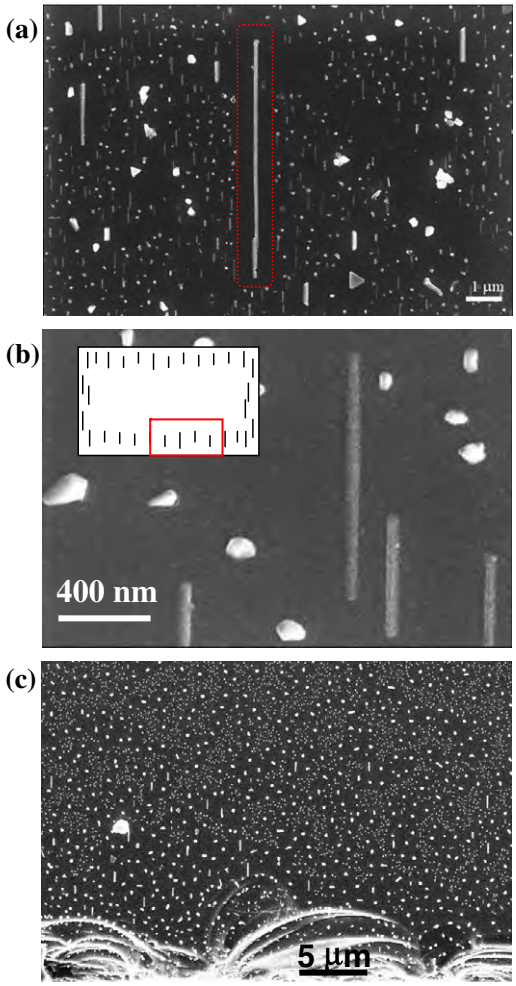

Figure 1. (a) SEM picture of the self-aligned carbon nanosticks processed by PLD growth. (b) Carbon nanosticks at higher magnification. Inset: a sketch is given that shows that the CNS only grow very close to the sample edges which is presented in (c) as an SEM image.

mechanism (more than the gas flow direction, propagation of the plasma or set-up geometry) which will be discussed in a subsequent chapter of this paper.

For further investigation atomic force microscopy (AFM) measurements were made with the CNS and one example is shown in figure 3(a). One advantage of AFM measurements compared to SEM inspection is the additional height information of the detected structures. Such two height profiles are presented in figures 3(b) and (c). Figure 3(b) shows the profile across one CNS and (c) the profile along the same CNS. In agreement with the SEM inspection presented in figure 1(b) the measured profile along the CNS exhibits a non-uniform height profile of the CNS. Further information for the growth mechanism can be obtained by determining the aspect ration of the CNS meaning the length of the CNS divided by their width. The aspect ratios of many CNS are presented in figure 3(d). It indicates an increased aspect ratio for longer CNS but with a trend to saturate for very long ones as it might be expected according to the growth model described below.

Electrical measurements were used to determine the conductivity of the CNS with the aim to probe their metallic or semiconducting nature. CNS were contacted by electron beam lithography using predefined markers. One example of such a contacted CNS is shown in figure 4(a) (SEM picture was made after the electrical measurements). A 4 μm long and 100 nm wide CNS was contacted with 5 nm Ti and 50 nm Au as electrodes for source and drain contacts and a separate gate. Many wires were destroyed during the contacting and parts of them looked like being evaporated verified by final SEM inspection. We assume the build up charges in the piezoelectric, pyroelectric and non-conductive substrate to be responsible for the damage at least providing some evidence of the non-isolating nature of the CNS.

In figure 4(b) conductivity measurements (source–drain current as a function of source–drain voltage for two different settings of gate voltage) at room temperature of a contacted CNS are shown for different values of gate voltages. The conductivity measurements were performed under ambient conditions and it needs to be mentioned that the results of the conductivity measurements of the CNS contacted were not completely reproducible. For some CNS contacted the conductivity changed between each two measurements and also showing sometimes a hysteresis. The lack of reproducibility can be explained either by the existence of surface charges but also by electromigration induced atomic rearrangement as described by Huang *et al* [8]. Despite the fact that the absence of any gate voltage dependence on the conductivity of a carbon nanowire (e.g. single walled carbon nanotube) usually indicates a metallic-like property of the system, here, the low gate capacitance needs to be taken into account. By making the approximation of a plate capacitor where the capacitance C is defined by $C = \varepsilon_0 \varepsilon_r A/d$ with ε_0 the dielectric constant, $\varepsilon_r = 1$ (air), $A \approx 4 \times 10^{-6}$ m $\times$ 5×10^{-8} m and $d \approx 5 \times 10^{-6}$ m for the device presented in figure 4(a) the gate capacitance is approximately $C_g \approx 0.35$ aF. This is 50 times smaller than gate capacitances of the standard Si/SiO_2 system used usually for these kind of measurements. Considering this small influence of the gate voltage on the conductivity of the device it cannot be stated if the nanosticks have a metallic or semiconducting characteristic.

Therefore, different characterization techniques than conductivity measurements are desirable.

To gain further information whether the CNS material is crystalline or amorphous transmission electron microscopy or nano-Raman spectroscopy would be helpful. Both characterization methods were addressed but no conclusion could be drawn due to substrate related preparation difficulties.

3. Model for self-aligned growth process

In the following we propose a model for the self-aligned growth process based on the experimental investigations presented in this paper. A major parameter controlling the growth process is diffusion. This statement is based on the existence of a capture zone [7] around each CNS as being visible in figure 1(a), a rather uneven surface topology as detected by AFM measurements (figure 3(c)) and the evolution of the aspect ratio (see figure 3(d)). Therefore, during the PLD process the ablated carbon atoms and clusters arrive first

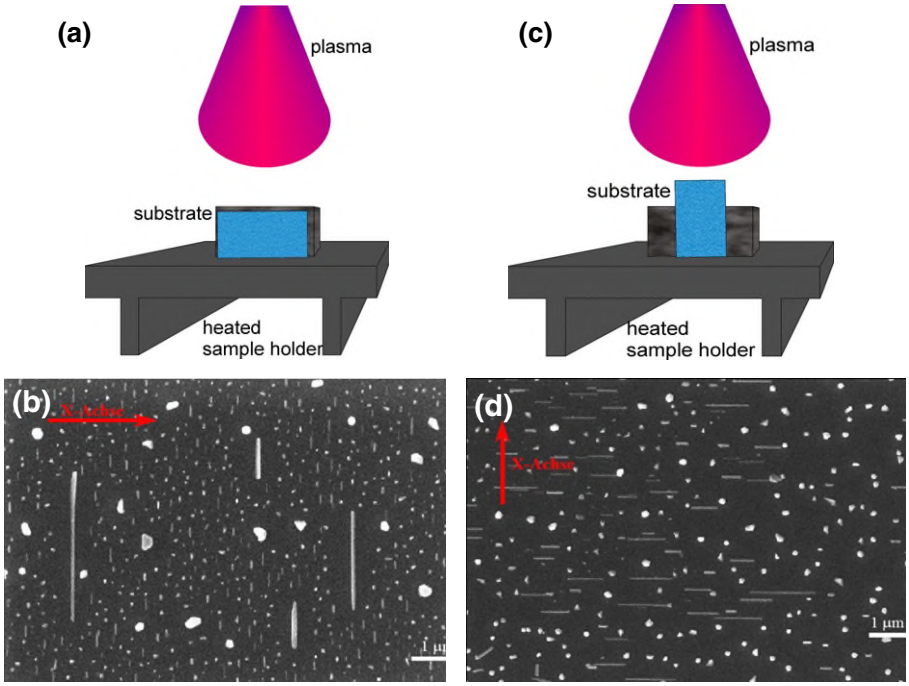

Figure 2. (a) and (b): set-up and results of growth on horizontally glued substrate to heated sample holder; (c) and (d) set-up and results of vertical substrate orientation.

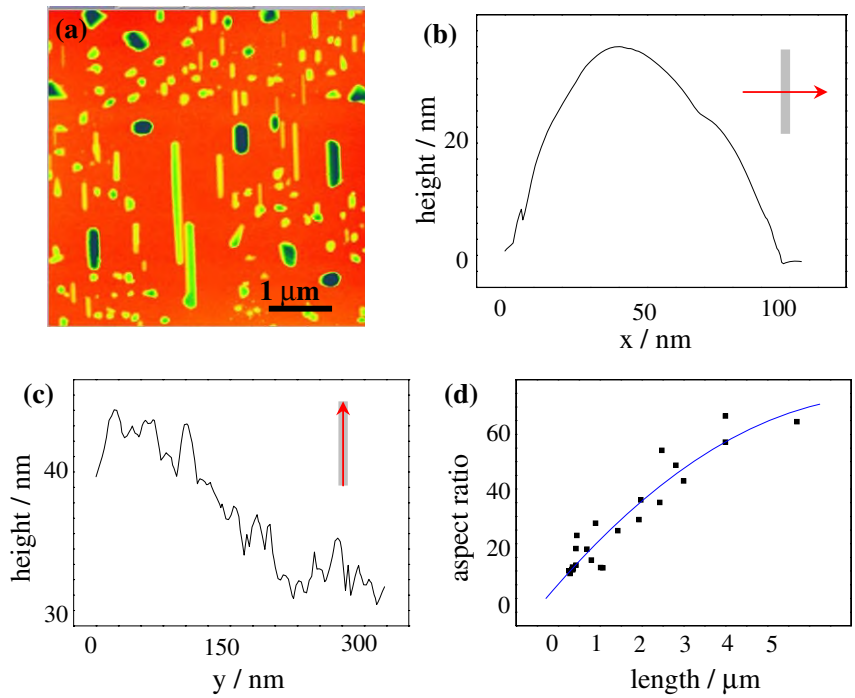

Figure 3. (a) AFM picture of the CNS (b) height profile of one CNS: measured across the CNS (c) height profile of one CNS: measured along the CNS (d) aspect ratio (length/width) of the CNS as a function of length.

on the substrate surface followed subsequently by a diffusion controlled growth process. The reason for the self-alignment can be found in the substrate properties. This assumption was proved for example by the experiments presented in figure 2. Apart from being a strong piezoelectric material, $LiNbO_3$ is also pyroelectric and due to the experimental set-up this pyroelectricity plays an important role. The $LiNbO_3$ substrate is glued to a sample holder in the PLD chamber and is heated (see figure 2). The heating process is not homogeneous and therefore pyroelectric fields build up on the substrate surface. The larger the temperature difference the larger the electric fields. Therefore, it can be assumed

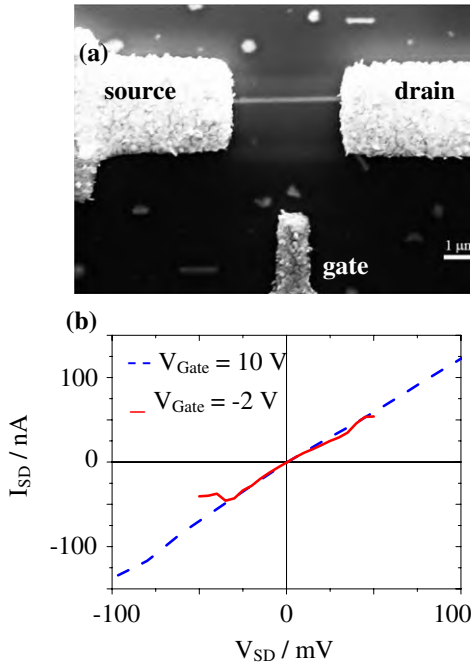

Figure 4. (a) SEM picture of a contacted CNS, (b) two conductivity measurements at room temperature of the contacted CNS.

that the largest fields are at the substrate edges. This agrees well with our observation that only at the sample edge CNS growth was initiated (as sketched as an inset in figure 1(b)). Furthermore, the CNS predominantly grow normal to the substrate X-axis. The substrate is $LiNbO_3$ (rotation 128°, Y-cut, X propagation) which is mainly used for surface acoustic wave propagation in X-direction because the Y-axis exhibit the largest piezoelectricity and pyroelectricity.

Based on the facts that the growth process is diffusion controlled and assisted by strong electric fields we hence propose the following growth model: impurities and crystal defects act as seeds for the carbon nanostructure growth and the first carbon clusters start to grow at these seed positions [10]. Due to the large electric fields close to the substrate edge the clusters become polarized. This strong polarization leads to a preferential agglomeration of further carbon at the most strongly polarized edges of the nanostructures finally leading to a self-aligned growth perpendicular to the substrate X-axis. A schematic sketch of this electric-field-guided growth process is presented as an inset in figure 5. This electric-field-guided growth mechanism has for example been used to grow carbon nanotubes in a preferential direction by applying electric fields during the DC plasma-enhanced CVD process [11]. By changing the direction of the applied electric field during the growth process also the growth direction of the carbon nanotubes was changed. The strength of the electric field inside the plasma sheath on the sample surface was estimated to be 5.14×10^5 V m^{-1}.

In the following we make an estimation if the electric field induced by the pyroelectric effect could be large enough to cause the self-aligned growth of the CNS which is based on a work by Rosenblum *et al* [9]. They investigated the electric field in $LiNbO_3$ samples created by the pyroelectric

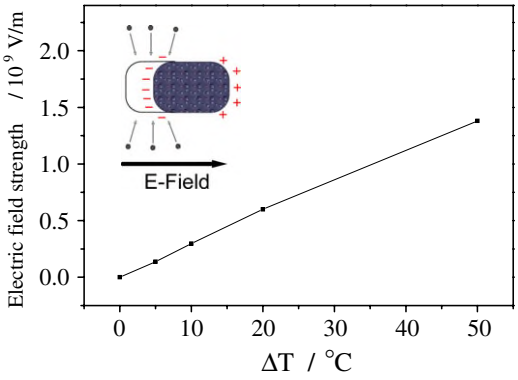

Figure 5. Calculated electric field induced by a temperature gradient across the pyroelectric substrate (after [9]). Inset: schematic sketch of the polarization of the CNS and the resulting orientated growth process.

effect and were able to show that the field can be as high as $|E_0| = 1.35 \times 10^9$ V m^{-1}, high enough for stimulated field emission of electrons. A temperature gradient in a pyroelectric material induces a finite polarization P_S which leads to an electric field at the sample surface $|E_0| = 4\pi|P_S|$. After [9], this polarization can be calculated using the expression:

$$\frac{3}{2}\left(\frac{P_S}{P_0}\right)^2 = -1 + \sqrt{1 + \frac{3}{4}\left[\frac{T_C - T}{\Delta T_0}\right]} \qquad (1)$$

with $T_C \sim 1200\,°C$ the Curie temperature for $LiNbO_3$, $P_0 = 0.71$ C m^{-2} and $\Delta T_0 = 90\,°C$. For a change in temperature from $T = 25$ to $100\,°C$ this results in a strength of the electric field of $|E_0| = 1.35 \times 10^9$ V m^{-1}. In figure 5 the calculated electric field is shown using (1) for a temperature gradient across the sample taking into account the averaged sample growth reference temperature of $T = 600\,°C$ (see table 1). According to the electric field strength estimation from [9] already a temperature difference across the substrate of $\Delta T = 0.03\,°C/5$ mm $= 6\,°C$ m^{-1} would be sufficient for the electric-field-guided growth process presented in [11]. Due to our sample growth set-up (see figure 2) where only one part of the substrate material is glued to the heated sample holder we assume to have a much larger temperature difference on the sample surface. Even though these estimations are not accurate it can be concluded that the electric fields induced by the pyroelectric substrate properties are large enough for the proposed self-aligned growth mechanism.

4. Summary

In summary, we have found a self-organized and self-aligned growth mechanism of carbon nanosticks by laser ablation of carbon on the substrate material $LiNbO_3$. Based on our experimental investigations and findings, we propose a model for the self-aligned growth. The main components of this growth process are diffusion and the piezo and pyroelectric substrate properties. Because the carbon nanostick structures are highly attractive for nanoelectronic applications, further investigations of the microscopic structure of the carbon nanosticks would be desirable.

Acknowledgments

The authors like to thank J K N Lindner for the attempts in transmission electron microscopy and A Hartschuh for the attempts in nano-Raman spectroscopy. We would also like to thank Alladin Ullrich for the help with the AFM pictures. Financial support of the German Excellence Initiative via the 'Nanosystems Initiative Munich (NIM)' is gratefully acknowledged.

References

[1] Li W Z, Xie S S, Qian L X, Chang B H, Zou B S, Zhou W Y, Zhao R A and Wang G 1996 *Science* **274** 1701
[2] Wei B Q, Vajtai R, Jung Y, Ward J, Zhang R, Ramanath G and Ajayan P M 2002 *Nature* **416** 495
[3] Huang M H, Mao S, Feick H, Yan H, Wu Y, Kind H, Weber E, Russo R and Yang P 2001 *Science* **292** 1897
[4] Hu J, Odom T W and Lieber C M 1999 *Acc. Chem. Res.* **32** 435
[5] Arepalli S and Scott C D 1999 *Chem. Phys. Lett.* **302** 139
[6] Rohlfing E A 1988 *J. Chem. Phys.* **89** 6103
[7] Cherepanov V and Voigtländer V 2004 *Phys. Rev.* B **69** 125331
[8] Huang J Y *et al* 2006 *Nano Lett.* **6** 1699
[9] Rosenblum B, Bräunlich P and Carrico J P 1974 *Appl. Phys. Lett.* **25** 17
[10] Förster A 2003 Physical vapor deposition *Fundamentals of Nanoelectronics* Forschungszentrum Jülich GmbH, Germany
[11] AuBuchon J F, Chen L-H, Gapin A I and Jin S 2006 *Chem. Vapor Depos.* **12** 370